nature biotechnology

Quantitative chemical proteomics reveals mechanisms of action of clinical ABL kinase inhibitors

Marcus Bantscheff[1,3], Dirk Eberhard[1,3], Yann Abraham[1], Sonja Bastuck[1], Markus Boesche[1], Scott Hobson[1], Toby Mathieson[1], Jessica Perrin[1], Manfred Raida[1], Christina Rau[1], Valérie Reader[2], Gavain Sweetman[1], Andreas Bauer[1], Tewis Bouwmeester[1], Carsten Hopf[1], Ulrich Kruse[1], Gitte Neubauer[1], Nigel Ramsden[2], Jens Rick[1], Bernhard Kuster[1] & Gerard Drewes[1]

We describe a chemical proteomics approach to profile the interaction of small molecules with hundreds of endogenously expressed protein kinases and purine-binding proteins. This subproteome is captured by immobilized nonselective kinase inhibitors (kinobeads), and the bound proteins are quantified in parallel by mass spectrometry using isobaric tags for relative and absolute quantification (iTRAQ). By measuring the competition with the affinity matrix, we assess the binding of drugs to their targets in cell lysates and in cells. By mapping drug-induced changes in the phosphorylation state of the captured proteome, we also analyze signaling pathways downstream of target kinases. Quantitative profiling of the drugs imatinib (Gleevec), dasatinib (Sprycel) and bosutinib in K562 cells confirms known targets including ABL and SRC family kinases and identifies the receptor tyrosine kinase DDR1 and the oxidoreductase NQO2 as novel targets of imatinib. The data suggest that our approach is a valuable tool for drug discovery.

Studies of drug action classically assess biochemical activity in settings that typically contain only the isolated target. Regularly, recombinant enzymes or protein fragments are used instead of the full-length endogenous proteins. To correlate accurately the activity of a compound determined in such assays with pharmacodynamic efficacy remains a challenge[1]. One reason for this discrepancy is that an isolated recombinant protein may not reflect the native conformation and activity of the target in its physiological context, because of the absence of interacting regulatory proteins, expression of alternative splice variants, incorrect protein folding or post-translational modifications. As a consequence, results from *in vitro* experiments may not predict the effects of a compound or drug in cells or *in vivo*. Moreover, although drugs are traditionally optimized against a single protein, many compounds act on multiple targets[2]. These 'off-targets' may increase the therapeutic potential of a drug, but they may also cause toxic side-effects.

Protein kinases represent an important class of drug targets, particularly in oncology and inflammation[3]. However, kinase drug discovery epitomizes the shortcomings of the single-gene/single-protein/single-assay paradigm, as kinase inhibitors can be both conformation specific and have multiple targets, as demonstrated by recently launched multi-kinase drugs[4–7]. Evidently, compounds directed at the ATP-binding site of kinases are not likely to be specific for a single kinase, because humans have around 500 protein kinases and more than 2,000 other purine-binding proteins that share similar binding pockets[8,9]. Conventional drug discovery mostly relies on panels of recombinant enzymes and cellular model systems to address compound potency, selectivity and potential off-target liabilities rather than attempting to determine the bona fide targets of a drug directly in an unbiased manner[10,11].

Recent progress in affinity-based proteomic strategies has enabled the direct determination of protein-binding profiles of small-molecule drugs under more physiological conditions[12]. To date, methods rely on the attachment of labels to the compound (immobilization, fluorescent or affinity tags) or to the proteins[10,13,14], which may introduce artifacts driven by the altered properties of the compound or the protein. Here we describe a chemical proteomics methodology that (i) captures a large portion of the expressed kinome and related proteins on a mixed kinase-inhibitor matrix (kinobeads) and (ii) subsequently analyzes this defined subproteome by quantitative mass spectrometry (MS)[15]. This approach allows the parallel quantitative determination of protein-affinity profiles of kinase inhibitors in any cell type or primary tissue as well as the differential mapping of drug-induced changes of phosphorylation events on the captured subproteome. We apply the methodology to three drugs targeting the oncogenic BCR-ABL kinase, which induces chronic myelogenous leukemia[16–18].

RESULTS

Target profiling with immobilized kinase inhibitors

Affinity purification strategies combined with MS-based protein identification enable the identification of potential drug targets directly from cells or tissues[12,19]. We applied this strategy to a collection of >100 ATP-competitive kinase inhibitors, which include

[1]Cellzome AG, Meyerhofstrasse 1, D-69117 Heidelberg, Germany. [2]Cellzome UK Ltd., Chesterford Research Park, Cambridge CB10 1XL, UK. [3]These authors contributed equally to this work. Correspondence should be addressed to G.D. (gerard.drewes@cellzome.com) or B.K. (bernhard.kuster@cellzome.com).

Received 5 April; accepted 16 July; published online 26 August 2007; doi:10.1038/nbt1328

chemical scaffolds, research tool compounds, drug candidates in development, as well as approved drugs (**Supplementary Fig. 1** online and data not shown). Most of these compounds do not contain functional groups suitable for covalent coupling to an affinity matrix while preserving activity. To overcome this limitation, we synthesized analogs containing primary amino groups (see **Supplementary Table 1** online for chemical structures). After immobilization of the compounds, the beads were incubated with lysates of HeLa or K562 chronic myelogenous leukemia cells to allow protein binding. After separation of the beads from the lysate, bound proteins were eluted, digested with trypsin, and identified by MS. Representative kinase-binding profiles of 12 immobilized tool compounds and drugs are shown in **Supplementary Figure 1**. The data are represented as heat maps, using the number of spectrum-to-sequence matches as a measure for the amount of captured protein[20]. In cases where the known targets of the compounds are expressed in HeLa or K562 cells, these targets were frequently identified (**Supplementary Tables 1** and **2** online). In addition, novel potential targets were found. Some of the compounds interacted rather selectively with few kinase targets whereas others displayed low selectivity. For instance, the immobilized analogs of the epidermal growth factor receptor inhibitors gefitinib (Iressa) and lapatinib (Tykerb), or the ABL inhibitor imatinib, bind few other kinases beyond their known targets. In contrast, all of the tool compounds, and the analogs of the clinical compounds sunitinib (Sutent) and vandetanib (Zactima), bind many more kinases.

Kinobeads—a mixed kinase inhibitor affinity resin

Although the affinity profiles of immobilized compounds reveal novel target candidates, they are problematic for the validation of inhibitor selectivity for several reasons. For instance, the results obtained for the immobilized molecule may not relate directly to the original compound owing to altered potency and selectivity resulting from attachment of the linker. Moreover, the resulting binding profiles are biased toward abundant proteins, which are often only weakly affected in subsequent activity-based assays[13,14,21].

To overcome these limitations, we developed a different approach, which uses the immobilized broad-selectivity inhibitors as kinase capturing–tools to analyze the interaction of competing 'free' compound with their protein targets in solution. The method is based on measuring competition between the unmodified test compound and immobilized ligands for ATP-binding and related sites on proteins. An unbiased target profile would require a capturing ligand that binds all members of a target class of interest. A previously described method used immobilized ATP as the ligand[22]. However, in our experience this approach resulted in the capture of fewer than ten kinases and was instead dominated by the binding of heat shock proteins (data not shown). Building on the observations from the immobilized kinase inhibitors described above, we selected from the set of immobilized compounds those ligands that displayed little selectivity and interacted with kinases on different branches of the kinase phylogenetic tree. Following this rationale, a mixed inhibitor resin was created by immobilizing a combination of seven ligands. These mixed kinase inhibitor beads (kinobeads) captured a

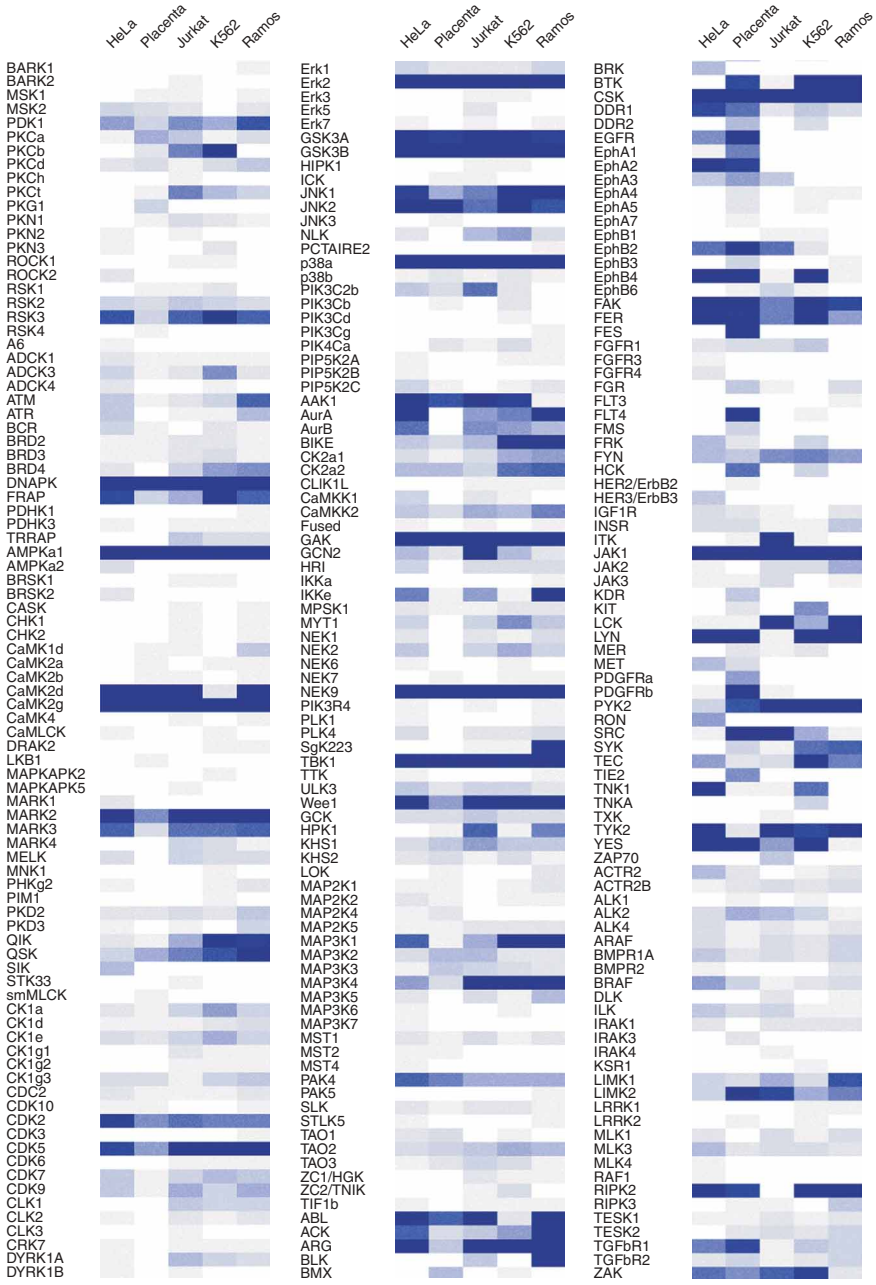

Figure 1 Kinobeads use immobilized kinase inhibitors as affinity reagents. Kinase profile of mixed kinase inhibitor beads (kinobeads). Seven broad-selectivity kinase inhibitors were immobilized and simultaneously exposed to lysates of human cell lines and primary tissue. Bound proteins were identified by MS. The number of spectrum-to-sequence matches was translated into a heat map as a semiquantitative indicator of the amount of protein captured.

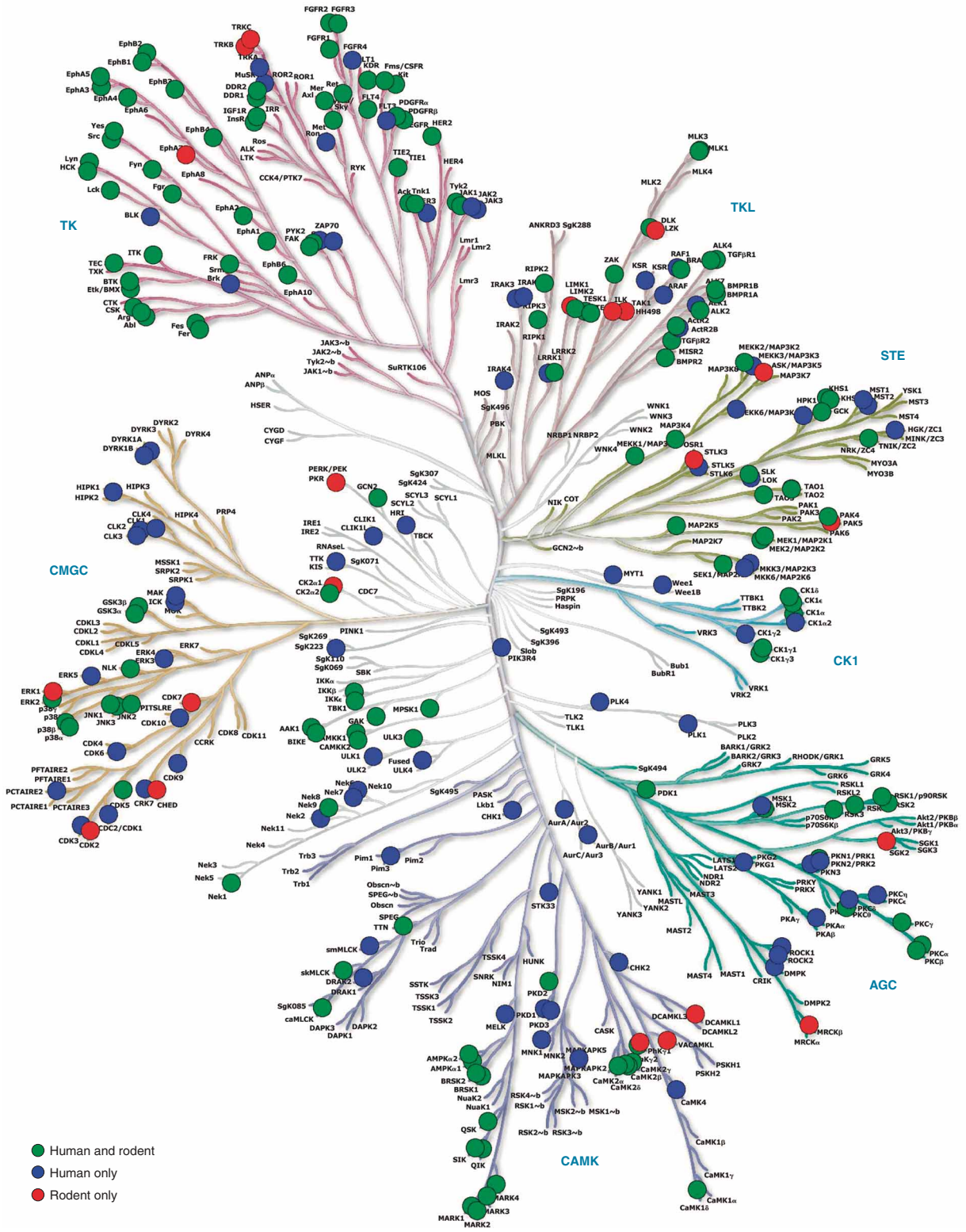

Figure 2 Kinobeads coverage of the kinome. Mass spectrometric analysis of kinobead purifications from 14 human and rodent cell lines and tissues (human HEK 293, HeLa, Jurkat, K562, Ramos, THP-1, kidney, placenta; mouse heart, liver, brain, muscle, kidney; and rat RBL-2H3) identified 307 kinases (269 human and 196 rodent) across all branches of the phylogenetic tree. Kinases that were found both in human and rodent samples are shown as green dots, whereas those specific for either human or rodent are shown in blue or red, respectively. Kinase tree adapted with permission from Cell Signaling Inc. (http://www.cellsignal.com/).

large portion of the expressed kinome. Using mass spectrometric analysis, a total of 174 and 183 protein kinases, from HeLa and K562 cells, respectively, were identified in single pull-down experiments, with a confidence interval for the identification set at 99% (**Fig. 1** and **Supplementary Table 3** online). When all the data obtained from kinobead pull-downs from 14 different human and mouse cell lines and tissues were accumulated, we identified a total of 307 nonredundant protein kinases (**Fig. 2**). Although slightly lower coverage was observed within the serine/threonine kinase branches compared to the tyrosine kinase branches, there were no major gaps.

Kinobeads not only capture protein kinases, but bind a defined subproteome consisting also of other ATP- and purine-binding proteins such as chaperones, helicases, ATPases, motor proteins, transporters and metabolic enzymes (**Table 1** and **Supplementary Table 3**). Based on the total mass spectrometric signal, we estimate that kinases account for almost 80% of the total captured protein amount (**Supplementary Fig. 2** online).

Target profiling of drugs in cell and tissue lysates

We applied kinobeads to the quantitative profiling of three inhibitors of the tyrosine kinase ABL. These were the drug candidate bosutinib (SKI-606), which is currently in clinical studies, and the marketed drugs imatinib and dasatinib[17,23,24]. All experiments were performed using K562 cells, which express the gene encoding the constitutively active BCR-ABL fusion protein[25]. The drugs were added to cell lysates in concentrations ranging from 100 pM to 10 μM and the lysates were subsequently subjected to kinobeads precipitation. When the drug in the lysate binds its target and thus blocks the ATP-binding site, a reduced amount of the free target is available for capturing on kinobeads, whereas the binding of nontargeted kinases and other proteins is unaffected (**Fig. 3a**). The kinobead-bound material from each spiking experiment was subjected to tryptic digestion and peptides were labeled with the different forms of the iTRAQ reagent[15]. Subsequently, peptide mixtures were combined and subjected to mass spectrometric peptide sequencing. Relative protein quantification was achieved by measuring the signal of the iTRAQ reporter ions relative to vehicle-treated lysate. From this data set, dose-response binding profiles were computed for >500 proteins in each sample, including ~150 kinases (**Supplementary Table 4** online).

For imatinib, 13 proteins exhibited >50% binding reduction on kinobeads at 1 μM drug concentrations in the lysate. These proteins include ABL/BCR-ABL (50% inhibitory concentration (IC_{50}) = 250 nM), the ABL family kinase ARG (IC_{50} = 272 nM) and two novel target candidates: the receptor tyrosine kinase DDR1 (IC_{50} = 90 nM) and the quinone oxidoreductase NQO2 (IC_{50} 43 nM) (**Fig. 3b** and **Supplementary Fig. 3** online). Note that our MS data do not reliably discriminate the normal ABL kinase expressed by the wild-type allele from the BCR-ABL fusion protein.

Although imatinib affected only three out of the 142 kinases that were quantified in the K562 lysate, dasatinib and bosutinib had broad target profiles (39 and 53 proteins, respectively, showed >50% competition at 1 μM), including the three imatinib targets BCR-ABL, ARG and DDR1 (**Fig. 3c** and **Supplementary Fig. 3**). The majority of the novel kinase targets were not available in commercial kinase panels, but enzyme activity assays for six tyrosine kinases (BTK, EphB4, focal adhesion kinase (FAK, also known as PTK2), FER, MER and SYK) and three serine/threonine kinases (GCK, KHS1 and p38a) gave IC_{50} values that generally support the kinobeads data (**Table 2**). A notable exception is FAK, which was affected only by bosutinib, consistent with published data reporting no binding of dasatinib or imatinib to FAK in phage-display studies[10,26]. However, a fraction of FAK corresponding to an activated conformation (detected by spectra of a diphosphorylated peptide representing the activation segment of the FAK kinase domain) was strongly affected by dasatinib, suggesting

Table 1 Number and functional categorization of proteins captured on kinobeads from human cell lines and tissue

Family	Subfamilies	HeLa	Placenta	Jurkat	K562	Ramos
Protein kinases	TK	37	52	36	38	29
	TKL	21	21	20	23	23
	STE	23	20	17	21	21
	CK1	4	4	6	6	6
	AGC	9	13	15	11	10
	CAMK	16	13	20	18	20
	CMGC	20	16	26	21	23
	Atypical	13	8	11	13	13
	TIF1	1		1	1	1
	Other	29	18	29	29	37
	Total	**173**	**165**	**181**	**181**	**183**
Lipid kinases	–	4	5	2	6	4
Sugar kinases	–	5	2	4	4	3
Nucleotide kinases	–	3	4	2	6	4
Other kinases	–	3	4	1	3	2
Enzymes	GTPases	2	4	4	3	4
	Helicases	20	5	14	16	20
	Hydrolases	76	105	81	108	128
	Isomerases	19	18	7	24	19
	Ligases	40	19	33	45	52
	Lyases	10	13	8	15	12
	Motor proteins	8	6	7	10	13
	Oxidoreductases	48	66	43	62	66
	Proteases	1	7	0	0	0
	Peroxidases	7	11	6	11	8
	Phospholipases	0	1	0	1	1
	Transferases	72	57	58	69	92
	Glucosidases	1	1	1	1	0
	Phosphatases	1	2	1	1	2
	Phosphodiesterases	4	6	4	2	4
	Ubiquitin ligases and proteases	6	2	4	7	7
	Total	**315**	**323**	**271**	**375**	**428**
Heat shock proteins	–	14	17	16	21	21
Nucleic acid binding	Purine metabolism	14	6	15	12	12
	Pyrimidine metabolism	3	3	3	4	3
	Ribosomal proteins	24	24	21	47	40
	Transcription factors	39	25	41	49	61
	Translation factors	31	18	22	29	35
	Others	55	47	48	53	77
	Total	**166**	**123**	**150**	**194**	**228**
Protein binding	Cytoskeleton	27	33	19	25	30
	Enzyme inhibitors	16	29	14	14	22
	GTPase regulators	17	16	21	22	30
	Kinase regulatory subunits	17	10	15	15	23
	Receptor binding	18	31	19	25	20
	Others	192	200	200	218	277
	Total	**287**	**319**	**288**	**319**	**402**
Transporters	–	82	108	87	89	130
Receptors	–	24	48	35	24	50
Lipid binding	–	9	14	10	13	15
Vesicle trafficking	–	8	19	8	7	14
Others or unknown	–	160	140	143	162	281
Total		**1,253**	**1,291**	**1,198**	**1,404**	**1,765**

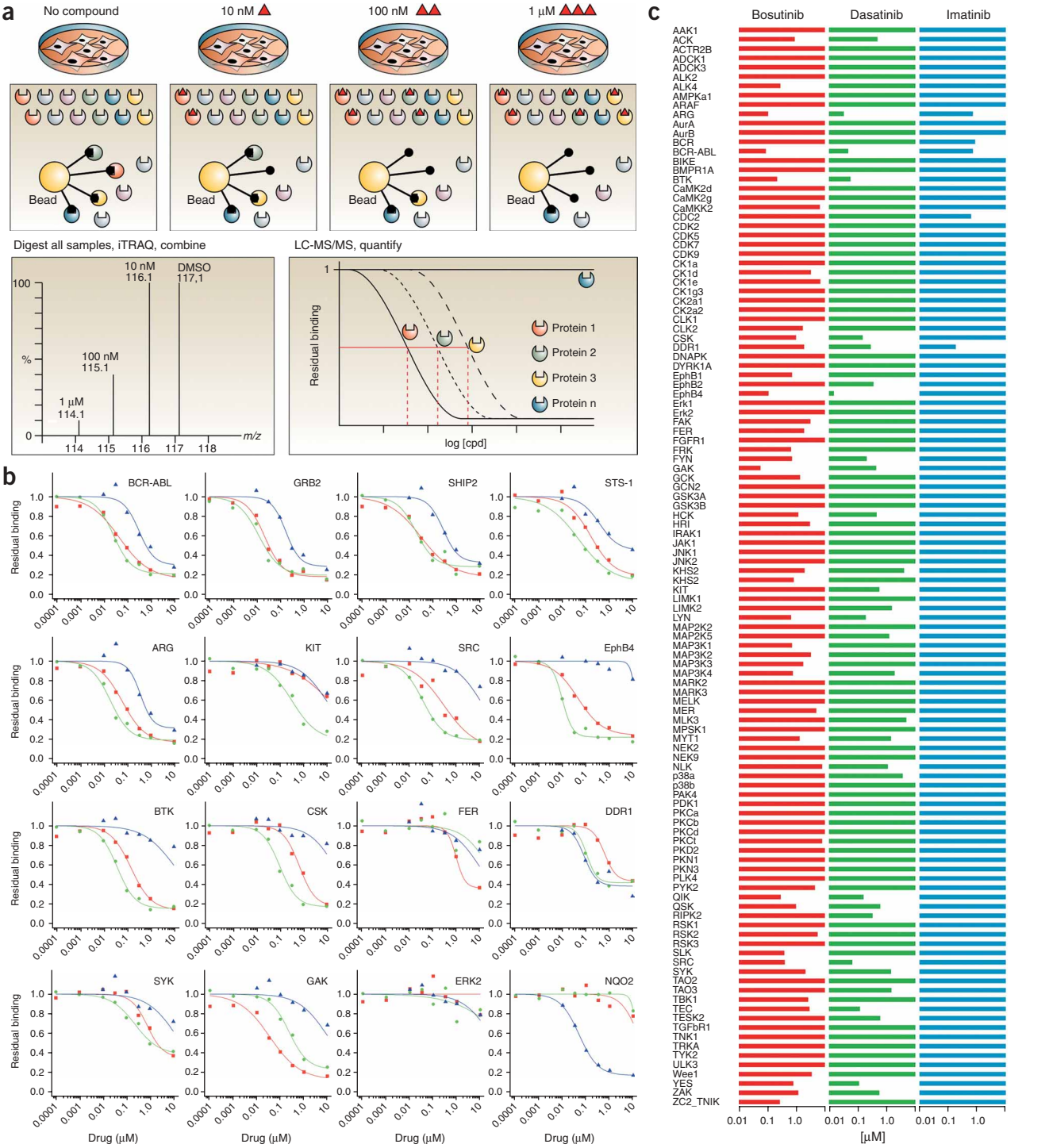

Figure 3 Proteomic profiling of drugs in cell lysate by a kinobeads competition assay. (**a**) Schematic overview of the kinobeads assay. Either lysates or cells are treated with vehicle and with compound over a range of concentrations (upper panel). Subsequently, proteins are captured on kinobeads. The 'free' inhibitor competes with the immobilized ligands for ATP-binding or related ligand-binding sites of its targets (middle panels). Bound proteins are digested with trypsin and each peptide pool is labeled with iTRAQ reagent (not shown). All four samples are combined and analyzed by MS. Each peptide gives rise to four characteristic iTRAQ reporter signals (scaled to 100%) indicative of the inhibitor concentration used (bottom left panel). For each peptide detected, the decrease of signal intensity compared to the vehicle control reflects competition by the 'free' compound for its target (bottom right panel). (**b**) Examples of competition binding curves calculated from iTRAQ reporter signals. Binding of several known and novel targets to kinobeads depends on the addition of imatinib (blue), dasatinib (green) and bosutinib (red) to K562 cell lysate. For each compound, three independent quadruplexed experiments (vehicle plus three compound concentrations each) were performed in duplicates, and iTRAQ reporter signal data were combined to display the dose response over nine concentrations. (**c**) Kinase-binding profiles of the ABL inhibitors imatinib (upper panel), dasatinib (middle panel), and bosutinib (bottom panel) across a set of protein kinases simultaneously identified from K562 cells. The bars indicate the IC_{50} values, defined as the concentration of drug at which half-maximal competition of kinobead binding is observed.

Table 2 IC_{50} values (nM) or inhibition (%) determined in biochemical enzyme assays

	Compound		
Purified kinase assayed	Imatinib	Dasatinib	Bosutinib
ARG[a]	500	NA	NA
BCR-ABL[a]	250	3.0	1.0
BTK	4% at 5 μM	1.1	2.5
CSK[a]	NA	NA	310
DDR1[b]	31 (22)	ND (7)	ND (12)
DDR2[c]	112	133	4,900
EphB4	5% at 5 μM	3.7	5.5
FAK	2% at 5 μM	0.2	1.0
FER	14% at 5 μM	36% at 5 μM	129
FYN[a]	NA	0.2	NA
GCK	10% at 5 μM	60% at 5 μM	9.9
KHS1	14% at 5 μM	22	0.3
KIT	13% at 1 μM	13	NA
LYN[a]	NA	3.0	8.0
MER	11% at 5 μM	40% at 5 μM	15.7
p38a	31% at 5 μM	867	1,400
SRC[a]	NA	0.5	1.0
SYK	38% at 5 μM	440	52
YES[a]	NA	0.4	NA

All values were determined by the Invitrogen "SelectScreen" service except as noted. [a]Published data (Investigational Drugs Database, Current Drugs 2007, http://www.iddb.com/). [b]Inhibition of autophosphorylation given in parenthesis (**Supplementary Methods** online). [c]Data generated by the Upstate IC_{50} Profiler Express service http://www.upstate.com/discovery/services/ic50_profiler.q. NA, not available; ND, not determined.

that the drug binds selectively to this activated conformation (**Supplementary Fig. 4** online). In agreement with this interpretation, dasatinib potently inhibited the activity of purified recombinant FAK.

In addition to kinases, several nonkinase targets were identified (**Supplementary Table 4**), some of which do not contain obvious small-molecule binding sites and hence are likely to bind drugs indirectly. Proteins that reside in a complex with the drug target are expected to exhibit similar competition behavior. Indeed the BCR-ABL interacting proteins GRB2, SHC1 and SHIP2 displayed similar competition behavior. STS-1, an adaptor protein described to inhibit the ubiquitin ligase CBL[27], also showed a similar dose-response for all three drugs. Consequently we propose it as a BCR-ABL kinase–interacting protein (**Fig. 3b**, top row).

In addition to the ABL kinases, imatinib is also known to inhibit oncogenic mutants of the KIT and platelet-derived growth factor (PDGF) receptors, which is the basis of its therapeutic application in gastrointestinal stromal tumors[28]. PDGF receptors are not expressed in K562 cells[29]. Although K562 cells do express wild-type KIT, no substantial competition of imatinib for kinobead-captured KIT was detected by MS. Likewise, bosutinib did not substantially affect KIT, but dasatinib showed potent binding (IC_{50} = 0.30 μM). This observation was confirmed by western blot analysis of the kinobead-captured material from imatinib-treated lysates using KIT antibodies (**Fig. 4a**). However, when the same blots were probed for activated KIT using a phospho-specific antibody directed against tyrosine 703, submicromolar competition by imatinib was seen. Hence, the kinobead-binding assay can differentiate among binding of a drug to distinct conformations of a target present in the same cell.

DDR1 and NQO2 are novel targets of imatinib

The discoidin domain receptor DDR1 represents a potential imatinib target. We confirmed the dose-response established by MS by probing the same samples with DDR1 antibodies (**Fig. 4a**). Next, we tested whether imatinib inhibits DDR1 kinase activity. DDR1 is a receptor tyrosine kinase that exhibits autophosphorylation and

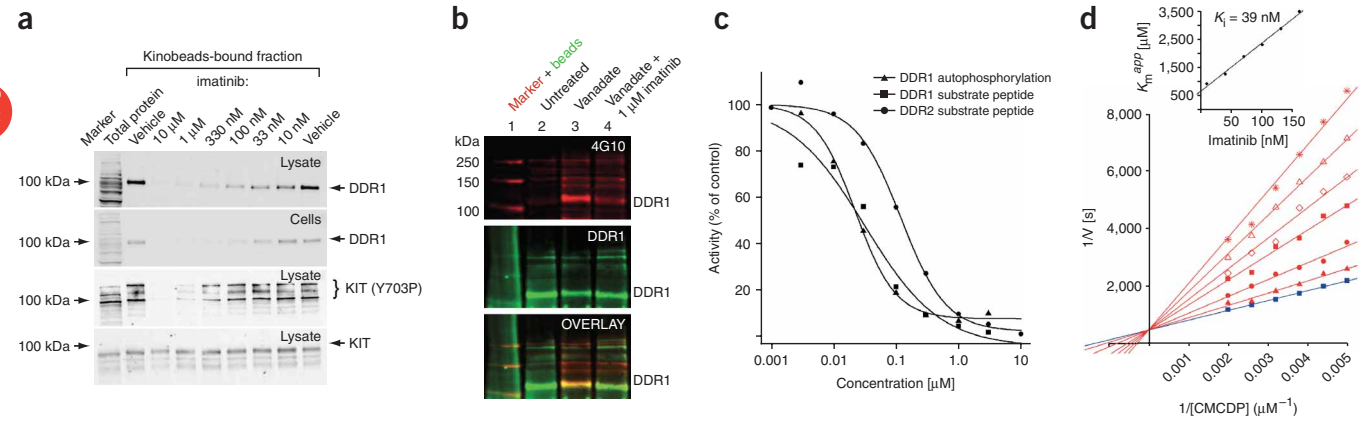

Figure 4 Targets of imatinib. (**a**) Western blot analysis of proteins captured on kinobeads. Imatinib treatment of K562 lysate reduces the amount of DDR1 captured on kinobeads (top panel). Imatinib treatment of K562 cells in culture similarly reduces the amount of DDR1 captured on kinobeads (second panel). Use of a phosphorylation-specific Y703P-KIT antibody (third panel) and a general KIT antibody (bottom panel) shows that only the Y703P-KIT species are affected by imatinib. The different mobilities of the Y703P-KIT bands may reflect differential phosphorylation and/or ubiquitination. (**b**) Inhibition of DDR1 autophosphorylation in K562 cells by imatinib. Cells were treated with pervanadate to induce tyrosine autophosphorylation of DDR1. DDR1 was analyzed by immunoprecipitation and western blotting with antiphosphotyrosine antibodies (4G10, upper panel) and DDR1 antibodies (middle panel). Preincubation of the cells with imatinib (lane 4) reduces the pervanadate-induced tyrosine phosphorylation and phosphorylation-mediated degradation of DDR1 (lane 3). (**c**) Imatinib is a potent inhibitor of the tyrosine receptor kinases DDR1 and DDR2. The enzymatic activity of a purified recombinant fragment of human DDR1 containing the cytoplasmic kinase domain was measured in radiometric assays of DDR1 autophosphorylation (triangles, IC_{50}= 22 nM) and the activity toward a substrate peptide (squares, IC_{50} = 31 nM). Imatinib also inhibits the only human DDR1 paralog, DDR2 (circles, IC_{50} = 112 nM). (**d**) Imatinib is a potent competitive inhibitor of the oxidoreductase NQO2. Recombinant human NQO2 was assayed spectrophotometrically in a coupled redox reaction using menadione as substrate, the nicotinamide analog CMCDP as cosubstrate, and MTT as indicator. Competitive inhibition is demonstrated by determining apparent K_m values for the cosubstrate at different imatinib concentrations (K_i = 39 nM, see inset).

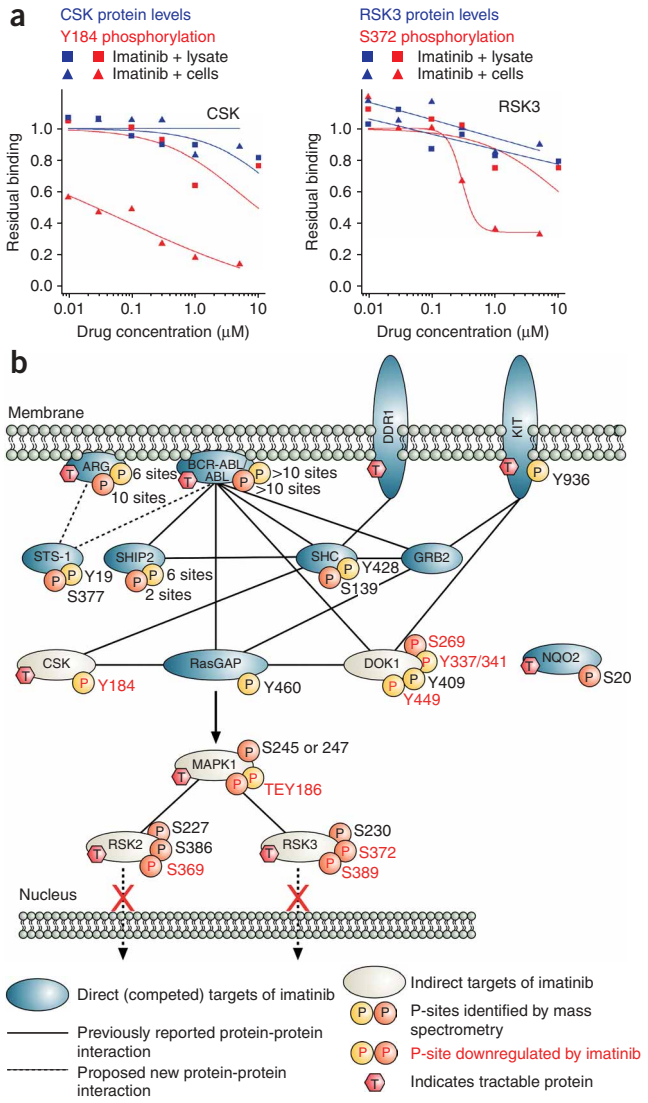

Figure 5 Phosphorylation analysis of kinobead-captured proteins to assess targets and downstream effects of imatinib. (**a**) Dose-dependent reduction of regulatory phosphorylation sites in imatinib-treated K562 cells (triangles) or lysates (squares) of regulatory sites on Csk (upper left panel) and RSK2 (bottom left panel). (**b**) Schematic representation of the proposed mechanism of action of imatinib in K562 chronic myelogenous leukemia cells. Direct targets (blue symbols) bind directly to the drug, or are associated in a complex with proteins directly binding and hence exhibit decreased binding to kinobeads in the presence of the drug. Indirect targets (white symbols) represent substrates of the direct targets. They do not bind directly to the drug and hence their binding to kinobeads is not affected, but they do exhibit reduced phosphorylation of potential or known regulatory sites. Imatinib binds to its direct target, which appears to be a BCR-ABL/GRB2/SHC/SHIP2/STS-1 complex, as imatinib (and also by dasatinib and bosutinib) competes with all of these proteins with similar characteristic potencies. Additional direct imatinib targets are the kinases ARG, DDR1 and KIT, and the oxidoreductase NQO2. Inhibition of the constitutively active BCR-ABL kinase downregulates the MAP kinase pathway and prevents nuclear entry and transcriptional activation of RSK kinases.

limited proteolysis in response to collagen binding or pervanadate treatment[30]. Preincubation of the cells with imatinib reduced tyrosine phosphorylation and proteolytic processing of DDR1 (**Fig. 4b**). Finally, we confirmed DDR1 as a potent imatinib target by measuring inhibition of the purified catalytic domain by means of autophosphorylation (IC_{50} = 22 nM) and the phosphorylation of a peptide substrate (IC_{50} = 31 nM, **Fig. 4c**). Consistent with the kinobeads data, all three drugs inhibit DDR1. Its only paralog, DDR2, is likewise inhibited by imatinib and dasatinib (**Table 2**).

The oxidoreductase NQO2 represents the first potential nonkinase target of imatinib. Although NQO2 represents the most prominent nonkinase protein captured from K562 cells, the binding to imatinib is specific, as dasatinib and bosutinib did not compete efficiently. None of the three drugs bind the closely related NQO1 isoenzyme. NQO2 is a cytosolic flavoprotein that catalyzes the metabolic reduction of quinones and related xenobiotics[31]. We tested the ability of imatinib to inhibit recombinant NQO2 in an enzyme assay measuring the reduction of menadione[32]. Imatinib displayed potent competitive inhibition with a K_i of 39 nM (**Fig. 4d**), in good agreement with the IC_{50} of 43 nM determined by kinobead binding, but itself was not modified by NQO2 (data not shown). Consistent with the kinobeads data, dasatinib and bosutinib did not inhibit NQO2.

Profiling of drug effects on signaling pathways

Potent kinase inhibitors typically exhibit slow off-rates, which permits a variation of the previous experimental strategy. Instead of adding the drugs to the lysate, we applied them over a range of concentrations to cultured cells 5 h before lysis and kinobeads precipitation. The results confirmed almost all of the targets obtained with the previous lysate competition experiments (**Supplementary Table 5** online). In a few cases, we observed competition when the compound was applied to cells, but not in the lysate competition experiment, for instance, in the case of imatinib and KIT (**Supplementary Fig. 5** online).

To explore not only the direct targets of the drugs but also their downstream effects on signaling pathways, we subjected aliquots of the iTRAQ-labeled peptide mixtures from kinobead precipitates to phosphopeptide enrichment and subsequent identification and quantification by MS. For imatinib-treated cells, 379 phosphorylation sites on 136 different proteins were identified. Eight of these sites on five different proteins exhibited substantial downregulation of their phosphorylation status in response to the drug (**Fig. 5a**). Indeed, most of these proteins have been implicated in signaling events downstream of ABL (**Fig. 5b**)[16,18]. For all three drugs together, we found downregulation of 20 sites on 13 proteins (**Supplementary Tables 6** and **7** online).

DISCUSSION

The catalytic domains of kinases display high structural homology. Therefore, an understanding of inhibitor selectivity in relevant tissues early in the process should increase the predictability of drug discovery, particularly for the application of kinase drugs in chronic conditions. Recently, techniques have been described to assess target profiles across the target class, ranging from affinity capturing of proteins in lysates using immobilized compounds to reactive ATP analogs[12,13,22,33]. Although these methods enable the mapping of binding proteins directly in tissue lysates, they have limited potential for drug discovery as they do not generate quantitative data. Therefore, the validation of inhibitor selectivity mostly relies on data from large assay panels using recombinant enzymes and enzyme fragments, which are then correlated with results from cell-based assays[10,26,34]. The kinobeads methodology described in this study enables quantitative, parallel profiling of the targets of drugs directed to the ATP-binding site directly in cells or in tissue lysate, without the need to modify either the compound or the proteins. The kinobeads matrix specifically captures ~200 protein kinases from any given cell type—estimated to represent at least two-thirds of the expressed

kinome[29]—and >600 additional chemically tractable proteins. Hence, a pharmacologically relevant subproteome becomes available for the study of drug binding and drug-induced changes such as post-translational modifications under near-physiological conditions. Single-target binding data can be recorded from the kinobeads with antibody reagents, enabling the screening of compounds against defined targets directly in tissue lysate. Moreover, recently developed multiplexed quantitative MS techniques[15] provide a comprehensive readout.

We validated this approach by profiling three ABL inhibitors and determined IC_{50} values in K562 lysate for several of their known targets, which are in line with reported cellular activities[23,35,36]. The obtained IC_{50} binding data are largely independent of the affinity of the targets for the immobilized ligands, because the effective concentration of capturing molecules is typically below the range of affinities of the competing compound for its targets[37]. Hence data obtained for all proteins in the same samples can be directly compared, which is an advantage compared with IC_{50} values determined in enzyme assays, which depend to a considerable degree on the assay conditions[34].

Our data propose novel kinase and nonkinase targets for all three drugs. Identification of only one novel kinase target of imatinib, the receptor tyrosine kinase DDR1, confirms the unusually high selectivity of this inhibitor. DDR1 is thought to play a role in tumor progression and metastasis, atherosclerosis, lung inflammation and fibrosis[38]. Activation of DDR1 inhibits p53-mediated apoptosis[39], possibly contributing to the synergetic effect of irradiation and imatinib treatment on tumor cell lines[40]. Although additional testing of imatinib in relevant disease models should further validate the role of DDR1 as a target, our data provide an interesting lead for further investigation. DDR1-knockout mice are resistant to bleomycin-induced lung fibrosis, a model in which imatinib shows efficacy[41,42].

A second unexpected target is the oxidoreductase NQO2, which protects cells against oxidative stress caused by xenobiotics[31]. High expression of NQO2 is found in myeloid cells, which are also the target of imatinib in chronic myelogenous leukemia. The potential consequences of NQO2 inhibition in patients treated with imatinib is beyond the scope of this study, but it is intriguing that the deletion of NQO2 in mice was reported to cause myeloid hyperplasia and this may be exacerbated in humans, where NQO1 deficiency is relatively common[31]. The second-generation ABL inhibitors dasatinib and bosutinib were developed as dual SRC/ABL kinase inhibitors and show overlapping but distinct target profiles. Bosutinib appears to be the first ABL inhibitor that does not inhibit KIT. As BCR-ABL upregulates KIT expression and stem cell factor responsiveness is associated with proliferation of leukemic stem cells[27], efficacy in chronic myelogenous leukemia might be impaired if KIT is not inhibited.

We identified many novel target candidates, and, where possible, confirmed them with biochemical assays. The potent inhibition of BTK and SYK, which signal downstream of immune receptors on granulocytes and B cells, predicts immunomodulatory potential, as has recently been demonstrated for dasatinib[43]. The physiological role of several other target candidates—for example, ACK/TNK2, GAK, QIK and QSK—is poorly understood. As all of these kinases potently bind to dasatinib and bosutinib at therapeutically relevant drug concentrations, they are likely to be affected during treatment. However, because these drugs appear to be relatively well tolerated, it can be inferred that the inhibition of these targets has no severe adverse consequences or may even contribute to efficacy.

For most targets, similar potencies were obtained by applying the compounds directly to cells in culture and by adding them to the lysate. A notable exception is the binding of imatinib to KIT, which was detected only when applied to cells in culture. This may be explained by two conformations existing in equilibrium in K562 cells, one of which binds imatinib. In the lysate, no competition was observed for the bulk of KIT, suggesting that the imatinib-binding form may amount to only a small fraction of total KIT. By contrast, when the drug was added to cultured cells, competition was observed for a substantial fraction of KIT. This suggests that imatinib effectively removes the high-affinity form from the equilibrium, leading to depletion of the form that does not bind imatinib. The high-affinity conformation is presumably represented by KIT phosphorylated at Y703 as this form, although present in only low amounts, was also competed with in the lysate (**Fig. 4a**). This observation is consistent with previous findings and with our enzyme assay data (**Table 2**) showing that imatinib does not effectively inhibit recombinant KIT[44]. The imatinib-binding phospho-form possibly mimics the conformation of the oncogenic KIT mutants, which represent the target of imatinib in gastrointestinal stromal tumors[17].

For a better prediction of drug effects it is useful to analyze the impact on the underlying signaling pathways. The mapping of drug-induced post-translational changes in the cellular kinome and its associated proteins can reveal effects of a drug beyond its direct targets. We find that a large portion of the BCR-ABL signaling pathway[16] is recapitulated in the kinobeads data (**Fig. 5b**). Imatinib binding to its direct target BCR-ABL results not only in the loss of BCR-ABL from kinobeads, but similarly reduces the amount of the associated signaling proteins GRB2, SHC and SHIP2. As STS-1 is reduced with similar dose-response characteristics, it may represent another member of the signaling complex. The inhibition of BCR-ABL leads to decreased tyrosine phosphorylation of the adaptors SHC (at Y427) and DOK1 (at several sites), and of the GTPase activating protein RasGAP (at Y460). In turn, MAP kinase is downregulated (at T184/Y186), leading to reduced phosphorylation of RSK kinases (at S360/377), which prevents nuclear translocation and the induction of transcription[45].

In conclusion, our quantitative chemical proteomic approach directly detects binding of small-molecule inhibitors to their targets in cells or tissue lysates and should be amenable to patient specimens such as tumor biopsies. Combination of the mixed-affinity matrix with quantitative MS provides a versatile tool to map a drug's direct and indirect targets in a single set of experiments. This approach should prove valuable at various stages of drug discovery as well as in translational studies of drug action in patient tissues.

METHODS

Kinobeads and competition assays. Reagents were purchased from Sigma unless otherwise noted. Compounds for immobilization to beads (**Supplementary Table 1**) were synthesized as described[46]. Kinobeads were prepared by immobilizing Bis-(III) indolyl-maleimide, purvalanol B, staurosporine and CZC8004, and the analogs of PD173955, sunitinib and vandetanib on NHS-activated Sepharose 4 beads (Amersham) as described[46]. Imatinib was purified from Gleevec tablets (Novartis) by high-performance liquid chromatography (HPLC). Dasatinib and bosutinib were synthesized following published procedures[47,48]. HeLa and K562 cells were obtained from ATCC and were cultured following ATCC protocols. Antibodies were purchased from Cell Signaling Technology (KIT, Y703P-KIT) and Santa Cruz (DDR1) and western blots were performed using a LI-COR Odyssey System.

Kinobeads profiling was performed essentially as described[46]. Additional details are also provided in the **Supplementary Methods** online. Briefly, cells were homogenized in lysis buffer (50 mM Tris/HCl pH 7.5, 5% glycerol, 1.5 mM $MgCl_2$, 150 mM NaCl, 20 mM NaF, 1 mM Na_3VO_4, 1 mM DTT, 5 μM calyculin A, 0.8% Igepal-CA630 and a protease inhibitor cocktail) using a Dounce homogenizer on ice. Lysates were cleared by centrifugation and

adjusted to 5 mg/ml protein concentration using the Bradford assay. Compounds were dissolved in dimethyl sulfoxide and added to 5 ml lysate samples, and 50 µl of a kinobeads suspension was added and agitated for 30 min at 4 °C. Subsequently, the beads were washed and collected by centrifugation, and bound material was eluted with SDS sample buffer and fractionated by SDS gel electrophoresis. For profiling of signaling pathways, compounds were added to 10^8 K562 cells per data point, grown at 10^6 cells/ml in RPMI/10% FCS. Beads were eluted with NuPAGE buffer, eluates were reduced, alkylated, separated on 4–12% NuPAGE gels (Invitrogen), and stained with colloidal Coomassie.

Mass spectrometry and data analysis. Procedures were essentially as described[46] and are detailed in the **Supplementary Methods** online. Briefly, gel lanes were cut into slices across the separation range and subjected to in-gel tryptic digestion[49], followed by labeling with iTRAQ reagents (Applied Biosystems) as described[15]. Labeled peptide samples were combined and phosphopeptides were enriched using immobilized metal affinity chromatography (PhosSelect, Sigma)[50]. Sequencing was performed by liquid chromatography–tandem mass spectrometry on an Eksigent 1D+ HPLC system coupled to a LTQ-Orbitrap mass spectrometer (Thermo Scientific). Peptide extracts of vehicle controls were labeled with iTRAQ reagent 117 and combined with extracts from compound-treated samples labeled with iTRAQ reagents 114–116 as detailed in **Supplementary Table 8** online. Tandem mass spectra were generated using pulsed-Q dissociation, enabling detection of iTRAQ reporter ions (see **Supplementary Data** and **Supplementary Tables 9–11** online). Peptide mass and fragmentation data were used to query an in-house curated version of the IPI database using Mascot (Matrix Science). Protein identifications were validated using a decoy database. iTRAQ reporter ion-based quantification was performed with in-house developed software. Curve fitting was performed using R software (http://www.r-project.org/).

Enzyme assays. DDR1 activation was assayed in K562 cells as described[30]. NQO2 activity was determined using purified recombinant human NQO2 with menadione as substrate and CMCDP (1-carbamoylmethyl-3-carbamoyl-1,4-dihydropyrimidine) as cofactor[32]. Kinase enzyme assays were performed as detailed in **Supplementary Methods** online.

Accession numbers. PRIDE database (http://www.ebi.ac.uk/pride): complete mass spectrometry data set accession numbers 2445-3178. IntAct molecular interaction database (http://www.ebi.ac.uk/intact): EBI-1379264, EBI-1380386, EBI-1380809, EBI-1380831 and EBI-1380874.

Note: Supplementary information is available on the Nature Biotechnology website.

ACKNOWLEDGMENTS

This work was partially supported by a grant from the German Bundesministerium fuer Bildung und Forschung (BMBF BioChancePLUS grant 0313335A). We would like to thank Charles Cohen, Tim Edwards, David Middlemiss, Markus Schirle, David Simmons and Francis Wilson for helpful discussions and support. We are grateful to Birgit Duempelfeld, Eva-Maria Kashammer-Lorenz, Jana Krause, Anja Podszuweit, Tatjana Rudi and Thilo Werner for expert technical assistance, to Svenja Burckhardt and Cyrille Boussard for the synthesis of compounds, to Michael Rinner, Judith Schlegl and Marianna Stabilini for database and IT tool development, and to Frank Weisbrodt for help with the figures. We would also like to thank Oliver Hantschel and Giulio Superti-Furga for stimulating discussions and valuable comments on the manuscript.

COMPETING INTERESTS STATEMENT

The authors declare competing financial interests: details accompany the full-text HTML version of the paper at http://www.nature.com/naturebiotechnology/.

Published online at http://www.nature.com/naturebiotechnology
Reprints and permissions information is available online at http://npg.nature.com/reprintsandpermissions

1. Hall, S.E. Chemoproteomics-driven drug discovery: addressing high attrition rates. *Drug Discov. Today* **11**, 495–502 (2006).
2. Morphy, R., Kay, C. & Rankovic, Z. From magic bullets to designed multiple ligands. *Drug Discov. Today* **9**, 641–651 (2004).
3. Cohen, P. Protein kinases–the major drug targets of the twenty-first century? *Nat. Rev. Drug Discov.* **1**, 309–315 (2002).
4. Liu, Y. & Gray, N.S. Rational design of inhibitors that bind to inactive kinase conformations. *Nat. Chem. Biol.* **2**, 358–364 (2006).
5. Daub, H., Specht, K. & Ullrich, A. Strategies to overcome resistance to targeted protein kinase inhibitors. *Nat. Rev. Drug Discov.* **3**, 1001–1010 (2004).
6. Mol, C.D., Fabbro, D. & Hosfield, D.J. Structural insights into the conformational selectivity of STI-571 and related kinase inhibitors. *Curr. Opin. Drug Discov. Devel.* **7**, 639–648 (2004).
7. Fabbro, D. & Garcia-Echeverria, C. Targeting protein kinases in cancer therapy. *Curr. Opin. Drug Discov. Devel.* **5**, 701–712 (2002).
8. Manning, G., Whyte, D.B., Martinez, R., Hunter, T. & Sudarsanam, S. The protein kinase complement of the human genome. *Science* **298**, 1912–1934 (2002).
9. Haystead, T.A. The purinome, a complex mix of drug and toxicity targets. *Curr. Top. Med. Chem.* **6**, 1117–1127 (2006).
10. Fabian, M.A. *et al.* A small molecule-kinase interaction map for clinical kinase inhibitors. *Nat. Biotechnol.* **23**, 329–336 (2005).
11. Fliri, A.F., Loging, W.T., Thadeio, P.F. & Volkmann, R.A. Analysis of drug-induced effect patterns to link structure and side effects of medicines. *Nat. Chem. Biol.* **1**, 389–397 (2005).
12. Szardenings, K., Li, B., Ma, L. & Wu, M. Fishing for targets: novel approaches using small molecule baits. *Drug Discov. Today: Technologies* **3**, 9–15 (2004).
13. Godl, K. *et al.* An efficient proteomics method to identify the cellular targets of protein kinase inhibitors. *Proc. Natl. Acad. Sci. USA* **100**, 15434–15439 (2003).
14. Knockaert, M. *et al.* Intracellular targets of cyclin-dependent kinase inhibitors: identification by affinity chromatography using immobilised inhibitors. *Chem. Biol.* **7**, 411–422 (2000).
15. Ross, P.L. *et al.* Multiplexed protein quantitation in *Saccharomyces cerevisiae* using amine-reactive isobaric tagging reagents. *Mol. Cell. Proteomics* **3**, 1154–1169 (2004).
16. Hantschel, O. & Superti-Furga, G. Regulation of the c-Abl and Bcr-Abl tyrosine kinases. *Nat. Rev. Mol. Cell Biol.* **5**, 33–44 (2004).
17. Capdeville, R., Buchdunger, E., Zimmermann, J. & Matter, A. Glivec (STI571, imatinib), a rationally developed, targeted anticancer drug. *Nat. Rev. Drug Discov.* **1**, 493–502 (2002).
18. Weisberg, E., Manley, P.W., Cowan-Jacob, S.W., Hochhaus, A. & Griffin, J.D. Second generation inhibitors of BCR-ABL for the treatment of imatinib-resistant chronic myeloid leukaemia. *Nat. Rev. Cancer* **7**, 345–356 (2007).
19. Ding, S. *et al.* Synthetic small molecules that control stem cell fate. *Proc. Natl. Acad. Sci. USA* **100**, 7632–7637 (2003).
20. Rappsilber, J., Ryder, U., Lamond, A.I. & Mann, M. Large-scale proteomic analysis of the human spliceosome. *Genome Res.* **12**, 1231–1245 (2002).
21. Wissing, J. *et al.* Chemical proteomic analysis reveals alternative modes of action for pyrido[2,3-d]pyrimidine kinase inhibitors. *Mol. Cell. Proteomics* **3**, 1181–1193 (2004).
22. Graves, P.R. *et al.* Discovery of novel targets of quinoline drugs in the human purine binding proteome. *Mol. Pharmacol.* **62**, 1364–1372 (2002).
23. Golas, J.M. *et al.* SKI-606, a 4-anilino-3-quinolinecarbonitrile dual inhibitor of Src and Abl kinases, is a potent antiproliferative agent against chronic myelogenous leukemia cells in culture and causes regression of K562 xenografts in nude mice. *Cancer Res.* **63**, 375–381 (2003).
24. Kantarjian, H., Jabbour, E., Grimley, J. & Kirkpatrick, P. Dasatinib. *Nat. Rev. Drug Discov.* **5**, 717–718 (2006).
25. Druker, B.J. *et al.* Effects of a selective inhibitor of the Abl tyrosine kinase on the growth of Bcr-Abl positive cells. *Nat. Med.* **2**, 561–566 (1996).
26. Carter, T.A. *et al.* Inhibition of drug-resistant mutants of ABL, KIT, and EGF receptor kinases. *Proc. Natl. Acad. Sci. USA* **102**, 11011–11016 (2005).
27. Kowanetz, K. *et al.* Suppressors of T-cell receptor signaling Sts-1 and Sts-2 bind to Cbl and inhibit endocytosis of receptor tyrosine kinases. *J. Biol. Chem.* **279**, 32786–32795 (2004).
28. Tuveson, D.A. *et al.* STI571 inactivation of the gastrointestinal stromal tumor c-KIT oncoprotein: biological and clinical implications. *Oncogene* **20**, 5054–5058 (2001).
29. Su, A.I. *et al.* Large-scale analysis of the human and mouse transcriptomes. *Proc. Natl. Acad. Sci. USA* **99**, 4465–4470 (2002).
30. L'hote, C.G., Thomas, P.H. & Ganesan, T.S. Functional analysis of discoidin domain receptor 1: effect of adhesion on DDR1 phosphorylation. *FASEB J.* **16**, 234–236 (2002).
31. Vella, F., Ferry, G., Delagrange, P. & Boutin, J.A. NRH:quinone reductase 2: an enzyme of surprises and mysteries. *Biochem. Pharmacol.* **71**, 1–12 (2005).
32. Knox, R.J. *et al.* Bioactivation of 5-(aziridin-1-yl)-2,4-dinitrobenzamide (CB 1954) by human NAD(P)H quinone oxidoreductase 2: a novel co-substrate-mediated antitumor prodrug therapy. *Cancer Res.* **60**, 4179–4186 (2000).
33. Patricelli, M.P. *et al.* Functional interrogation of the kinome using nucleotide acyl phosphates. *Biochemistry* **46**, 350–358 (2007).
34. Knight, Z.A. & Shokat, K.M. Features of selective kinase inhibitors. *Chem. Biol.* **12**, 621–637 (2005).
35. Buchdunger, E. *et al.* Inhibition of the Abl protein-tyrosine kinase *in vitro* and *in vivo* by a 2-phenylaminopyrimidine derivative. *Cancer Res.* **56**, 100–104 (1996).
36. Lombardo, L.J. *et al.* Discovery of N-(2-chloro-6-methyl-phenyl)-2-(6-(4-(2-hydroxyethyl)-piperazin-1-yl)-2-methylpyrimidin-4-ylamino)thiazole-5-carboxamide (BMS-354825), a dual Src/Abl kinase inhibitor with potent antitumor activity in preclinical assays. *J. Med. Chem.* **47**, 6658–6661 (2004).

37. Lowe, C.R., Harvey, M.J., Craven, D.B. & Dean, P.D. Some parameters relevant to affinity chromatography on immobilized nucleotides. *Biochem. J.* **133**, 499–506 (1973).
38. Vogel, W.F., Abdulhussein, R. & Ford, C.E. Sensing extracellular matrix: an update on discoidin domain receptor function. *Cell. Signal.* **18**, 1108–1116 (2006).
39. Ongusaha, P.P. *et al.* p53 induction and activation of DDR1 kinase counteract p53-mediated apoptosis and influence p53 regulation through a positive feedback loop. *EMBO J.* **22**, 1289–1301 (2003).
40. Rossler, J., Zambrzycka, I., Lagodny, J., Kontny, U. & Niemeyer, C.M. Effect of STI-571 (imatinib mesylate) in combination with retinoic acid and gamma-irradiation on viability of neuroblastoma cells. *Biochem. Biophys. Res. Commun.* **342**, 1405–1412 (2006).
41. Avivi-Green, C., Singal, M. & Vogel, W.F. Discoidin domain receptor 1-deficient mice are resistant to bleomycin-induced lung fibrosis. *Am. J. Respir. Crit. Care Med.* **174**, 420–427 (2006).
42. Daniels, C.E. *et al.* Imatinib mesylate inhibits the profibrogenic activity of TGF-beta and prevents bleomycin-mediated lung fibrosis. *J. Clin. Invest.* **114**, 1308–1316 (2004).
43. Kneidinger, M. *et al.* Dasatinib (BMS354825) inhibits IgE-dependent activation and histamine release in human blood basophils. *Blood* **108** Abs. 1365 (2006).
44. Shah, N.P. *et al.* Dasatinib (BMS-354825) inhibits KITD816V, an imatinib-resistant activating mutation that triggers neoplastic growth in most patients with systemic mastocytosis. *Blood* **108**, 286–291 (2006).
45. Yang, T.T., Xiong, Q., Graef, I.A., Crabtree, G.R. & Chow, C.W. Recruitment of the extracellular signal-regulated kinase/ribosomal S6 kinase signaling pathway to the NFATc4 transcription activation complex. *Mol. Cell. Biol.* **25**, 907–920 (2005).
46. Drewes, G. *et al.* Process for the identification of novel enzyme interacting compounds. Patent WO 2006/134056 A1 (2006).
47. Boschelli, D.H. *et al.* 7-Alkoxy-4-phenylamino-3-quinolinecar-bonitriles as dual inhibitors of Src and Abl kinases. *J. Med. Chem.* **47**, 1599–1601 (2004).
48. Das, J. *et al.* 2-aminothiazole as a novel kinase inhibitor template. Structure-activity relationship studies toward the discovery of N-(2-chloro-6-methylphenyl)-2-[[6-[4-(2-hydroxyethyl)-1-piperazinyl)]-2-methyl-4-pyrimidinyl]amino)]-1,3-thiazole-5-carboxamide (dasatinib, BMS-354825) as a potent pan-Src kinase inhibitor. *J. Med. Chem.* **49**, 6819–6832 (2006).
49. Shevchenko, A., Wilm, M., Vorm, O. & Mann, M. Mass spectrometric sequencing of proteins silver-stained polyacrylamide gels. *Anal. Chem.* **68**, 850–858 (1996).
50. Pozuelo, R.M., Campbell, D.G., Morrice, N.A. & Mackintosh, C. Phosphodiesterase 3A binds to 14–3-3 proteins in response to PMA-induced phosphorylation of Ser428. *Biochem. J.* **392**, 163–172 (2005).